Petrography, Geothermobarometry and Metamorphic History of Metapelites from the Central Ruby Range Southwest Montana

HAMELIN, Clémentine[1], BALDWIN, Julia A.[2], HARMS, Tekla A.[3], and BRADY, John B.[1]

[1] Department of Geosciences, Smith College, Northampton, MA 01063, chamelin@smith.edu, [2] Department of Geosciences, University of Montana, Missoula, MT 59812, [3] Department of Geology, Amherst College, Amherst, MA 01002

ABSTRACT

The Ruby Range is one of several uplifted Precambrian blocks in southwest Montana, near the northwestern margin of the Archean Wyoming province. It was metamorphosed during the Big Sky orogeny ~ 1.72-1.79 Ga (Baldwin et al., 2014; Cramer et al., 2013). This study seeks to characterize further the P-T metamorphic conditions of the Big Sky orogenic event as recorded in the central Ruby Range. Metapelite samples were collected during July 2014 as part of a Keck Geology Consortium summer research project. Garnet-biotite-sillimanite-bearing metapelite rocks associated with marble, amphibolite and metamorphosed banded iron formation were sampled from the Christensen Ranch Metamorphic Suite (CRMS) at the highest structural levels of the central Ruby Range near Stone Creek. Textures and mineral assemblages preserve evidence for partial melting. All samples contain the assemblage biotite + garnet + sillimanite +quartz, consistent with upper amphibolite to lower granulite facies metamorphism. Four samples were further investigated with petrographic observations, geochemical XRF and SEM/EDS analyses and modeling to determine *P-T* conditions and history recorded in the samples. A peak-temperature value of ~800°C at a pressure of 9kb and a second, possibly re-equilibrated *T,P* value of ~700°C and ~ 7 kbar was determined from further investigation of five samples. Quartz-in-garnet (QuiG) barometry was used to determine entrapment pressures of quartz grains includes in garnets, providing insight into the prograde metamorphic history of the metapelite samples from the CRMS, yielding peak-pressure results of ~12 kbar between ~700-800 °C. These results are consistent with the *P-T* conditions and metamorphic history for the Big Sky orogeny determined in the adjacent Tobacco Root Mountains (Cheney et al., 2002; Brady et al., 2004, Harms et al., 2004).

INTRODUCTION

- The Ruby Range is one of several Laramide uplifted blocks of exposed Precambrian basement in the Wyoming Province.
- Metamorphosed at 2.45 Ga and 1.72-1.79 Ga during the Big Sky Orogeny, (Harms et al., 2004; Cheney et al., 2004).
- This project examines metapelites along the Stone Creek drainage, from the structurally highest unit of the Ruby Range, the Christensen Ranch Metamorphic Suite (CRMS) overlying the Dillon Gneiss and Pre-Cherry Creek suite.
- CRMS only show Proterozoic monazite ages 1.72-1.79 Ga (Cramer et al., 2014)
- The purpose of this study is to determine metamorphism conditions of pressure and temperature recorded in these metapelites to further constrain and understand the Big Sky orogeny as recorded in the Ruby Range, complementing our understanding of this orogenic event studied in the adjacent mountain ranges such as the Tobacco Root Mountains or the Gravelly Range.
- Petrography, mineral chemistry and thermodynamic modeling.

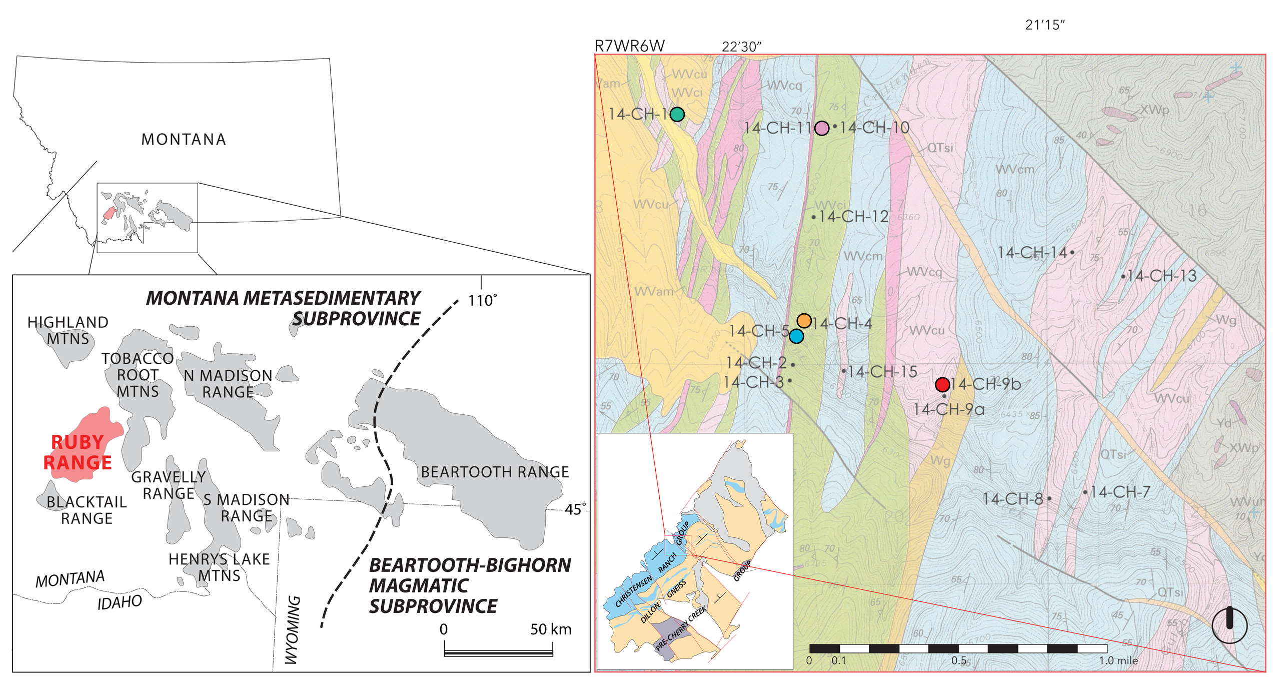

Figure 1. Sample distribution and location map along Stone Creek. Metapelite samples were generally sampled in the undifferentiated metasedimentary units (mapped in pink), a few samples were collected in the amphibolite unit (mapped in green). Other units mapped are calcitic and dolomitic marbles (blue), metamorphosed banded iron formation (purple) and quartzite (magenta). Note the contact with the Dillon gneisses (olive green) to the left of the map. (Modified from James, 1990).

METHODS

- 21 metapelite samples collected in summer of 2014 for KECK project, along Stone Creek drainage, structurally covering base to top of the CRMS (Figure 1).
- All samples have mineral assemblage garnet + biotite + sillimanite + quartz. Outcrop and sample positions recorded in NAD 84 UTM coordinates using a GPS. Samples and field relationships with surrounding units were described in the field.

FOR PSEUDOSECTION GEOTHERMOBAROMETRY:

(1) 25 sections were made, phases, modes and reaction textures identified, described and quantified using a petrographic microscope.
(2) Bulk rock chemistry for major and trace elements (X-Ray Fluorescence, XRF) and REE (Inductively Coupled Plasma Mass Spectrometry, ICPMS) was obtained through Acme Labs, Vancouver Canada for 9 samples.
(3) 5 samples analyzed using and FEI Quanta 450 SEM with EDAX-EDS. Garnet, biotite and plagioclase mineral chemistry was quantified, modal phase maps were generated.

- Pseudosection modeling for 5 samples in Na-Ca-K-Fe-Mg-Al-Si-H-Ti-O (NCKFMASHTO) system with TheriakDomino v. 03.08.2009 & pelites (Holland and Powell dataset 5.5), for LOI water value vs. H_2O determined using a $T\text{-}X_{H2O}$ binary diagram calculated in Theriak Domino vs. 'wet'-addition modeling from 'wet' peraluminous granite (granite + 25% H_2O) No apatite correction was done, Mn was left out and small ferric iron values were used.
- Stable mineral assemblages, actual modes vs. calculated modes, and mineral compositions compared for LOI vs. $T\text{-}X_{H2O}$ determined H_2O value.
- Conventional geothermobarometry using Spear & Kohn's GTB program.
- Quartz-in-garnet (QuiG) barometry (Kohn, 2013), using GeobaRamanTry program.

RESULTS

PETROGRAPHY

- Schistose texture with well-developed foliation defined by abundant biotite and sillimanite grain alignment. Two samples with a gneissic texture, with higher feldspar + quartz content.
- Garnets: anhedral, range in size from 1 mm to 10 cm diameter. Generally Fe-rich (~80% almandine), little to no zoning, but with evidence for two garnet-growth episodes (inclusion free or different rims, Ca and Fe zoning in one sample).
- Biotite between dioctahedral and trioctahedral biotite, Fe-Mg ratios in biotite range from ~ 1:1 to 2:3 across samples but, generally consistent within samples.
- Generally muscovite-free, a few samples contain minor amounts of retrograde-muscovite.
- Kyanite and cordierite-absent.
- Most samples k-feldspar poor, only samples CH1, 9b and 11a contains abundant matrix k-feldspar.

MINERAL ASSEMBLAGES

grt + bt + sill + pl + qtz ± ap ± k-spar ± chl ± mu ± ilm ± ru ± gr ± trm.

Sample CH1

- fine-grained, homogeneous
- K-feldspar rich matrix
- garnet (Fe, Ca) and tourmaline (Ca) zoning
- Rare, single-grained garnet inclusions (bt, mu, qtz, apt)
- prismatic sillimanite in matrix

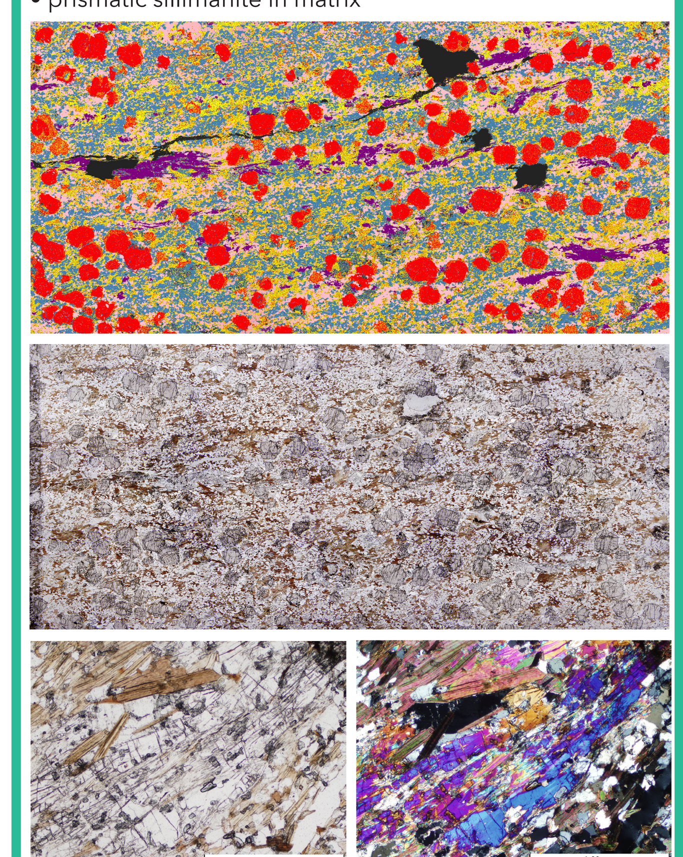

Garnets for QuiG barometry:

- preserved garnet zoning in CH1 garnets: high-Ca and low-Fe euhedral garnet cores (garnet growth 1), low-Ca and high-Fe garnet rims (garnet growth2) with quartz inclusions in both domains.

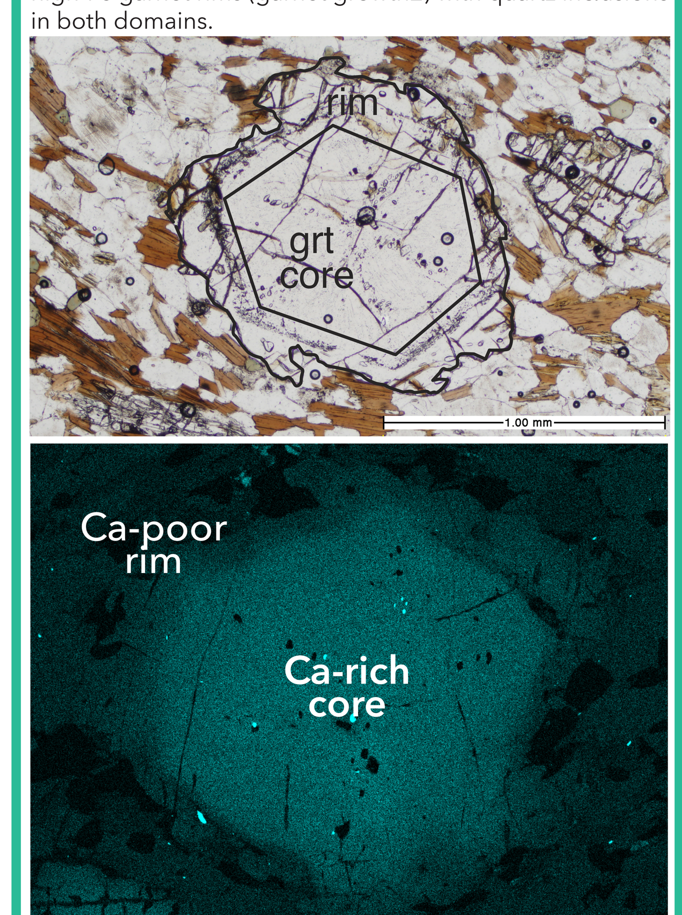

Figure 2. CH1 Sample Petrography: Phase maps, thin section maps and textural details - top: phase map and PPL thin section of CH1, prismatic sillimanite texture, PPL & XPL; bottom: two episodes of garnet growth, euhedral core and crinkled rim (XPL and Ca-zoning EDS map),

GEOTHERMOBAROMETRY

Conventional P-T (GTB) • Thermodynamic P-T modeling (Theriak-Domino) • QuiG Barometry (GeobaRamanTry)

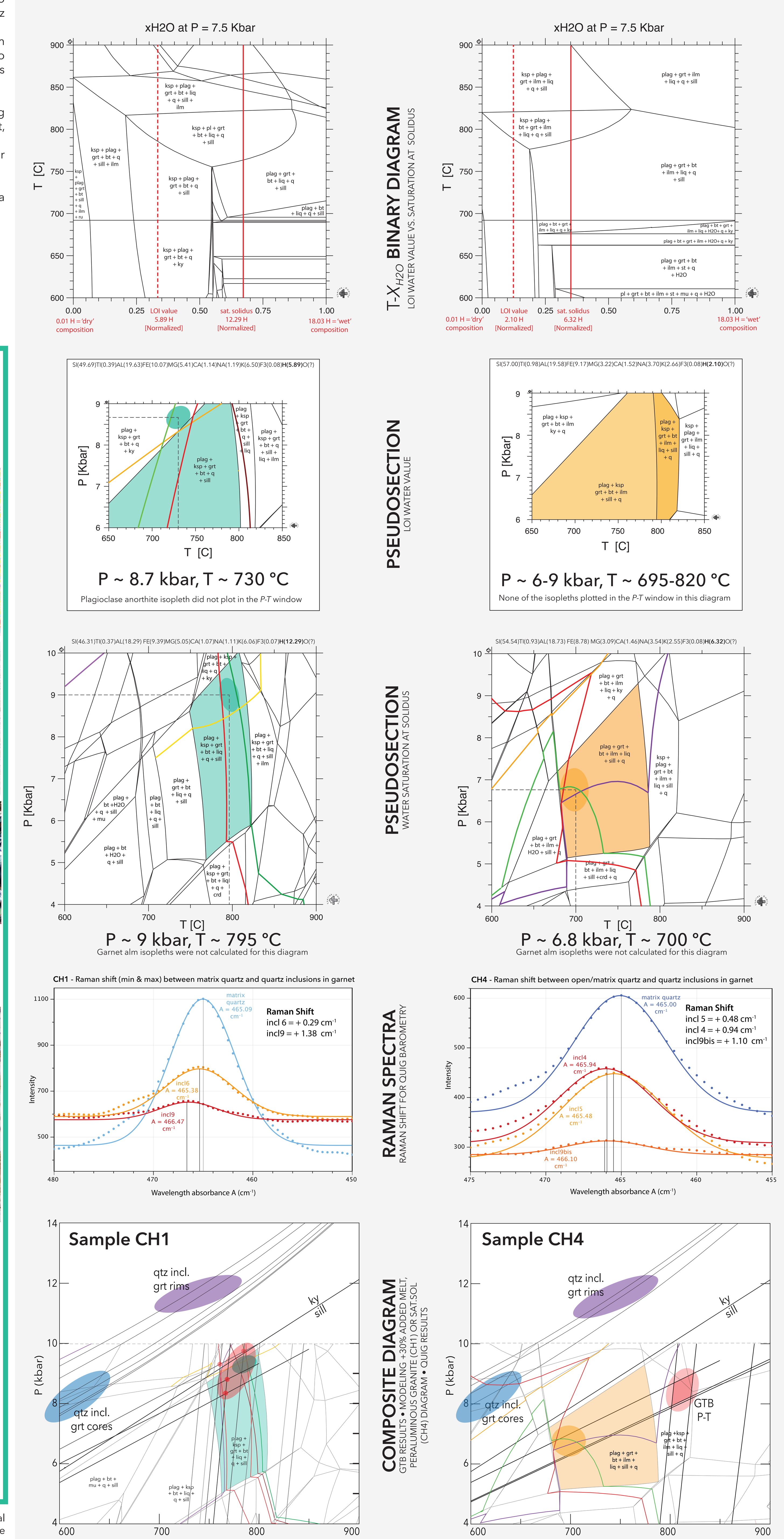

Figure 4. left column: CH1 results, right column, CH4 results. From top to bottom: a) $T\text{-}X_{H2O}$ diagrams a 7.5 kbar showing variations due to water content adjustments; b) Pseudosection using loss on ignition (LOI) water values,; c) Pseudosection using water saturation at solidus determined using a $T\text{-}X_{H2O}$ diagram for XRF bulk rock composition; d) Pseudosection with 30% added melt from a 'wet' peraluminous granite ; e) Raman spectra with quartz peak, showing Raman shift between matrix and included quartz grains; f) Combined geothermobarometry results (QuiG, conventional P-T, and 30%added melt combined diagram)

PSEUDOSECTION ISOPLETHS

- Garnet Mg/(Mg+Fe)
- Biotite Mg/(Mg+Fe)
- Garnet grossular Ca/(Fe+Mg+Ca)
- Garnet almandine Fe/(Fe+Mg+Ca)
- Plagioclase anorthite Ca/(Ca+Na+K)

PHASE MAPS - KEY

GARNET | PLAG | KSPAR | MAGN | RUTILE | BIOTITE | ILM | SILL | QTZ | APAT

Sample CH4

- medium to coarse grained, poikiloblastic garnet clusters around quartz + sillimanite melt pods.
- No K-feldspar, no muscovite in matrix
- Flat garnet profiles, no compositional zoning but clear inclusion domains.
- Kinked fibrous sillimanite bundles

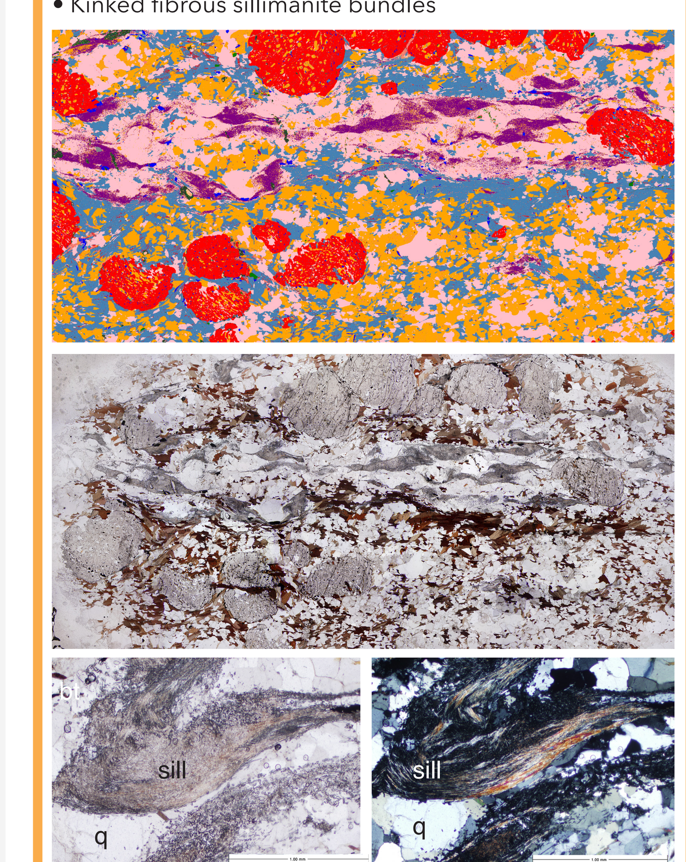

Garnets for QuiG barometry:

- Inclusions patterns indicative of two garnet growth episodes: plagioclase inclusions in cores vs. ilmenite inclusions in rims or ears, strong inclusion trails. quartz inclusions in both subdomains

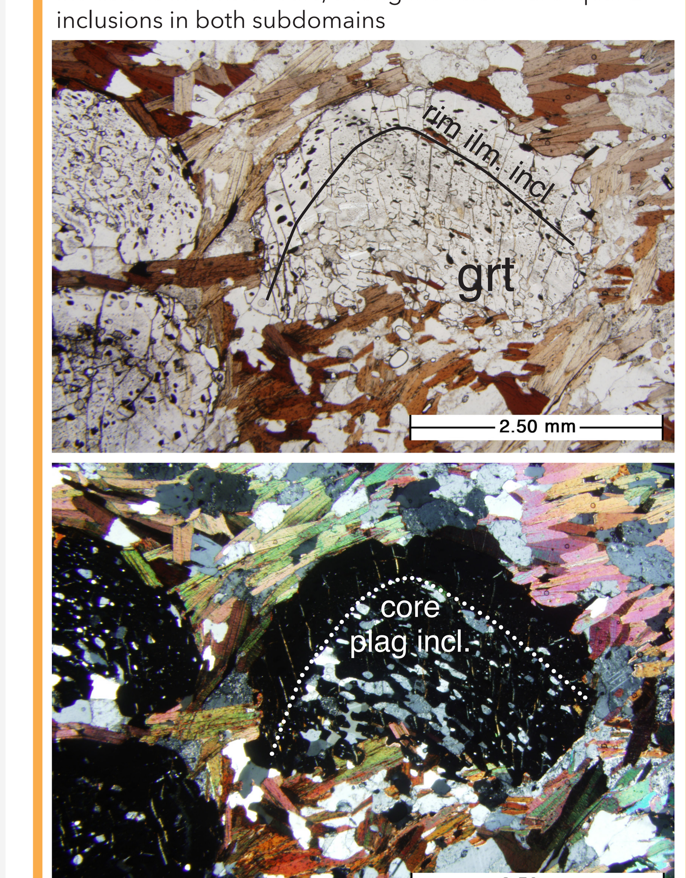

Figure 3. CH4 Sample Petrography: Phase maps, thin section maps and textural details - top: phase map and PPL thin section of CH1, fibrous sillimanite texture, PPL & XPL; bottom: two garnet growth episodes, plagioclase-free, ilmenite-rich rim inclusions (PPL) and plagioclase-rich core inclusions (XPL),

RESULTS

- Stable assemblage fields in mineral assemblage diagrams match petrography. Modeled (Theriak-Domino) vs. observed modes (SEM phase map) also match well for both LOI water value vs. H_2O saturation at solidus values (Table 1)
- Petrography: NKFMASH petrogenetic grid, preliminary constraints on *P,T* are 650 °C - 900 °C (muscovite-OUT, K-feldspar-IN), 2-11 kbar (cordierite and kyanite absent) (Figure 4, grey area).
- Further *P-T* constraint from conventional P-T and pseudosection modeling:
  ~700-800 °C and 7-9 kb (Figure 4),
  Peak-T at ~800 °C, ~8.5 kbar (CH1, CH9b, CH11a)
  Re-equilibration values at ~725 °C, ~7 kbar (CH4, CH5a)
- Overall, results from thermodynamic modeling consistent with mineral compositional analyses and determined modes, with some differences within *P-T* window (lower *P,T* vs. higher *P,T*). Some differences with conventional P-T results, but within the 700-80 °C, 7-9 Kbar window.
- QuiG barometry give insight into propage and peak-P garnet growth pressures, from ~8 kbar at ~600°C to ~12 kbar between 700-800 °C (peak-P).

PHASE	GARNET			BIOTITE			SILL.			QUARTZ			PLAG.			K-SPAR			ILMENITE		
modes (vol%)	LOI	H2O+	ROCK	LOI	H2O+	ROCK	LOI	H2O+	ROCK	LOI	H2O+	ROCK	LOI	H2O+	ROCK	LOI	H2O+	ROCK	LOI	H2O+	ROCK
CH1	17	16	19	28	33	31	3	5	3	23	24	21	10	8	7	20	16	17	0	0	0
CH4	18	12	13	10	19	23	5	6	5	31	33	30	28	26	24	7	0	0	1.4	1.2	0.7

Table 1. Phase mode comparison in samples for calculated LOI and H2O melt saturation at solidus modeling, and quantified phase modes (SEM/EDS phase map for CH1, CH4, CH9b; estimated modes for CH11a).

DISCUSSION

- Results plotted on NCKFMASH grid, within consistent range, but with some differences, which could be due to polymetamorphism (evidence for multiple episodes of garnet growth & consumption).
- All CRMS ages 1.72-1.79 Ga: *P-T* conditions recorded for Big Sky orogeny in the Ruby Range, not from metamorphic events at 2.45 Ga.

MODELING ISSUES & SOURCES OF DISCREPANCIES IN RESULTS

- Sources of error: a-x models, no Mn, no apatite correction, composition analyses, H_2O content, melt loss, polymeta morphism.
- If assume H_2O loss from dehydration melting reactions only (Spear et al., 1999), use LOI diagrams, no melt below 750-800 °C.
- Melt-loss not represented in the bulk rock chemistry: Melt addition show theoretical pre-melt loss sta bility fields, isopleths show matching compositions for added melt vs. LOI.
- Proposed *P-T* path for BSo (Fig.4).

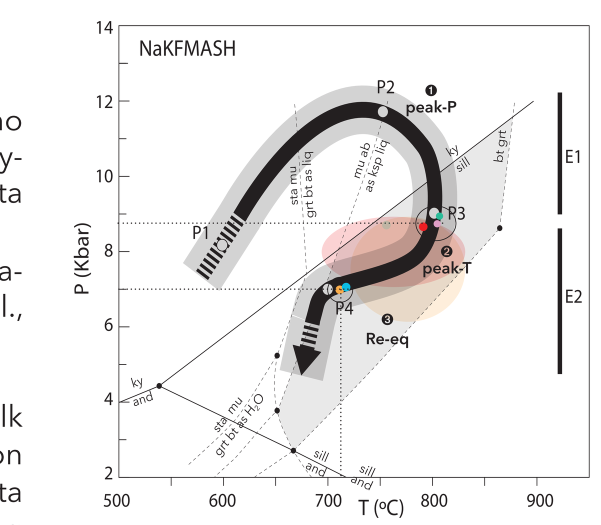

Figure 4. Proposed *P-T* bath for BSo on petrogenetic grid in NaKFMASH system for pelites. Light grey area = maximum *P-T* constraint from petrographic observations, colored spots = thermodynamic modeling *P-T* constraints + conventional *P-T*, colored triangles = QuiG barometry results. (Modified from Spear et al.,1999).

CONCLUSION & SIGNIFICANCE

- Implications for the Big Sky orogeny in the Ruby Range: constraint on peak-T, peak-P, and re-equilibrium P-T conditions.
- Calculated reequilibrium temperature of ~700 °C at pressure of ~7 kbar.
- Calculation results affected by bulk rock composition H_2O content estimations, mineral composition measurements, mineral a-x models, melt loss and polymetamorphism.
- Result for peak-T and peak-P for the Big Sky orogeny comaprable to result in the Tobacco Root Mountains, recorded in pelitic schists from the Indian Creek Metasedimentary Suite (Cheney et al., 2004) despite not being equivalent (ICMS 1st cycle vs. ICMS 2nd cycle metasediments).

ACKNOWLEDGEMENTS

I would like to thank my advisor, John B. Brady, for putting the time and energy in this project, for letting me make my own decisions about this research and giving me a sense of ownership in the work I am doing, making this an intensive learning and growing collaborative research experience. I am also extremely thankful to Julia A. Baldwin, for helping me with the Theriak Domino modeling and for giving me precious advice on how to think about rocks in the Ruby Range, in the field and in the lab; Tekla A. Harms for her patience and understanding with technical issues, eternal support and motivation to keep going and not get discouraged. I would also like to thank Jack Cheney at Amherst for K-feldspar staining, Frank Spear and his graduate students at RPI for inviting me to use the Raman spectrometer for QuiG, Mike Vollinger for the cookies and Judith Whopereis for her help and technical support with the SEM/EDS system. Finally, I would like to thank the KECK Geology Consortium and the Ruby Rangers, for making exciting research in the field and in the lab possible, and for fun times in Montana!

REFERENCES

- Baldwin, J.A., Cramer, M.A., Voarino, B., 2014, Late Archean to Paleoproterozoic evolution of the Ruby Range, Montana, and its implications for the growth and modification of the Northwestern Wyoming Province: Geological Society of America Abstracts with Programs, v. 46, No 5, p. 20.
- Cheney, J.T., Brady, J.B., *Tierney, K.A., *DeGraff, K.A., *Mohlman, H.K., *Frisch, J.D., *Hatch, C.E., *Steiner, M.L., *Tuit, C., *Steffan, K.J., *Cady, P., *Lowell, J., *Archuleta, L.L., *Hirst, J., *Carmichael, S.K., *Fisher, R.G.M., *Wegmann, K.W., and Monteleone, B. (2004) Proterozoic metamorphism of the Tobacco Root Mountains, Montana, in Brady, J.B., Burger, H.R., Cheney, J.T., and Harms, T.A., eds., Precambrian Geology of the Tobacco Root Mountains, Montana: Geological Society of America Special Paper 377, 105-129.
- Cramer, M.A., Voarino, B., and Baldwin, J.A. (2013) Metamorphic evolution of Precambrian basement in the southern Ruby Range, SW Montana in Geological Society of America Abstracts with Programs, 45, 601.
- De Capitani C. and Petrakakis K. (2010): The computation of equilibrium assemblage diagrams with Theriak/Domino software. American Mineralogist 95:1006-1016
- Harms, T.A., Brady, J.B., Burger, H.R, and Cheney, J.T. (2004) Advances in the geology of the Tobacco Root Mountains, Montana, and their implications for the history of the northern Wyoming Province, in Brady, J.B., Burger, H.R., Cheney, J.T., and Harms, T.A., eds. Precambrian Geology of the Tobacco Root Mountains, Montana: Geological Society of America Special Paper 377, p. 227-243.
- Kohn, M. J., (2014) "Thermoba-Raman-try": Calibration of spectroscopic barometers and thermometers for mineral inclusions: Earth and Planetary Science Letters 388, p 187-196.
- Powell, R, & Holland, TJB, 1988 An internally consistent thermodynamic dataset with uncertainties and correlations: 3: application methods, worked examples and a computer program. Journal of Metamorphic Geology 6, 173–204.
- James, H.J., (1990) Plate 1: Geologic map of the Southwestern Ruby Range, Montana in Precambrian Geology and Bedded Iron Deposits of the Southwestern Ruby Range, Montana: US Geological Survey Professional Paper 1495, 44.
- Spear, Frank A., Kohn, Matthew, J., Cheney, John T. (1999) P-T paths from anatectic pelites. Contributions to Mineralogy and Petrology 134: 17-32